

See discussions, stats, and author profiles for this publication at: <https://www.researchgate.net/publication/231229283>

Design of Supramolecular Layers via Self-Assembly of Imidazole and Carboxylic Acids

ARTICLE *in* CRYSTAL GROWTH & DESIGN · OCTOBER 2001

Impact Factor: 4.89 · DOI: 10.1021/cg000008k

CITATIONS

120

READS

50

3 AUTHORS, INCLUDING:



John C Macdonald

Worcester Polytechnic Institute

46 PUBLICATIONS 3,847 CITATIONS

SEE PROFILE



Pieter C Dorrestein

University of California, San Diego

200 PUBLICATIONS 5,985 CITATIONS

SEE PROFILE

Design of Supramolecular Layers via Self-Assembly of Imidazole and Carboxylic Acids

John C. MacDonald,* Pieter C. Dorrestein, and Malissa M. Pilley

Department of Chemistry, Northern Arizona University, Flagstaff, Arizona 86011-5698

Received September 5, 2000

ABSTRACT: The supramolecular chemistry and crystal structures of salts of imidazole with one monocarboxylic acid (**1**), nine different dicarboxylic acids (**2–10**), and one tetracarboxylic acid (**11**) are reported. Salts **2–11** serve as building blocks that self-assemble via ionic O–H \cdots O and N–H \cdots O hydrogen bonds when crystallized. These strong hydrogen bonds generate two types of chains that intersect at the anions and form polar hydrogen-bonded layers with four different motifs. These layers serve as scaffolds with which to control molecular packing in two dimensions for engineering the structures of crystals. All imidazolium cations function as multidentate proton donors by forming two or three C–H \cdots O hydrogen bonds in addition to two N–H \cdots O hydrogen bonds. Strong O–H \cdots O and N–H \cdots O hydrogen bonds define structure and connectivity within layers, while weaker C–H \cdots O hydrogen bonds dominate interactions between layers in these salts.

Introduction

Designing organic crystals that exhibit useful solid-state properties such as nonlinear optical behavior, electrical conductivity, and solid-state reactivity is not a trivial problem. For any one of these properties to occur, components must have the requisite molecular structure and molecular orientation within the crystal lattice.^{1,2} Organic synthesis has advanced to the point where we can design organic molecules with almost any desired structure and chemical properties. Despite recent progress toward understanding the molecular basis of crystal nucleation and processes that govern crystal growth,^{3,4} it still is difficult both to predict how molecules pack during crystallization and to control all of the intermolecular forces that determine patterns of molecular packing in organic crystals.

Currently, the most successful strategy for engineering the structures of crystals takes advantage of hydrogen-bonding interactions between molecules as the principal means to control molecular self-assembly during crystallization. This method takes advantage of the strong directing capability of hydrogen bonds to organize individual molecules into supramolecular aggregates that have well-defined structures. These supramolecular aggregates often have unique chemical and physical properties due to the collective behavior of these weakly bound molecules. Hydrogen bonds have been used to generate supramolecular assemblies of organic molecules with structures that can be controlled selectively in one and two dimensions.^{5–29} A common problem with many of these systems, however, is the tendency of organic compounds with several different functional groups to form more than one pattern of hydrogen bonds. For example, compounds that contain both carboxylic acid and primary amide functional groups self-assemble by forming two different types of hydrogen-bonded chains.³⁰ The motifs of these chains

differ depending on whether acid and amide groups form a combination of R₂²(8) acid–acid and amide–amide homodimers or just acid–amide heterodimers. Formation of two different hydrogen-bonding motifs in this manner can promote polymorphism that arises when the molecules pack in different arrangements during crystallization.^{31–33} From the standpoint of design, it is important to limit the occurrence of polymorphism, because polymorphs generally have physical properties that differ in ways that cannot be predicted.

This paper describes our efforts to control molecular packing in crystalline materials by using organic salts as molecular building blocks. One advantage in using organic salts rather than neutral organic molecules is that hydrogen bonds between ions generally are stronger than those between neutral molecules. Another advantage is that the ability of cations and anions to function as hydrogen-bonding donors or acceptors can be tuned using acid–base chemistry. Our strategy involves using organic salts that self-assemble into two-dimensional supramolecular networks, or layers. Constraining molecules to assemble into layers has several advantages from the standpoint of design and control over bulk crystalline structure: it significantly reduces the degrees of translational freedom available to individual molecules while packing; it limits molecular packing to just a few possible packing arrangements by defining the relative position and orientation of molecules within layers; it reduces the problem of predicting crystal packing in three dimensions from that of individual molecules to that of well-ordered layers of molecules.

We chose to investigate a series of salts between imidazole and dicarboxylic acids, **2–11** (Figure 1), as molecular building blocks for several reasons. Previous studies have shown that imidazole deprotonates carboxylic acids to form the corresponding imidazolium carboxylate salts.³⁴ Imidazolium carboxylate salts form hydrogen-bonded chains in which the ions are bonded together by strong ionic N–H \cdots O hydrogen bonds. These chains of alternating imidazolium cations and

* To whom correspondence should be addressed. Phone: 520-523-8893. Fax: 520-523-8111. E-mail: john.macdonald@nau.edu. Web: www.nau.edu/~chem/faculty/macdonald.

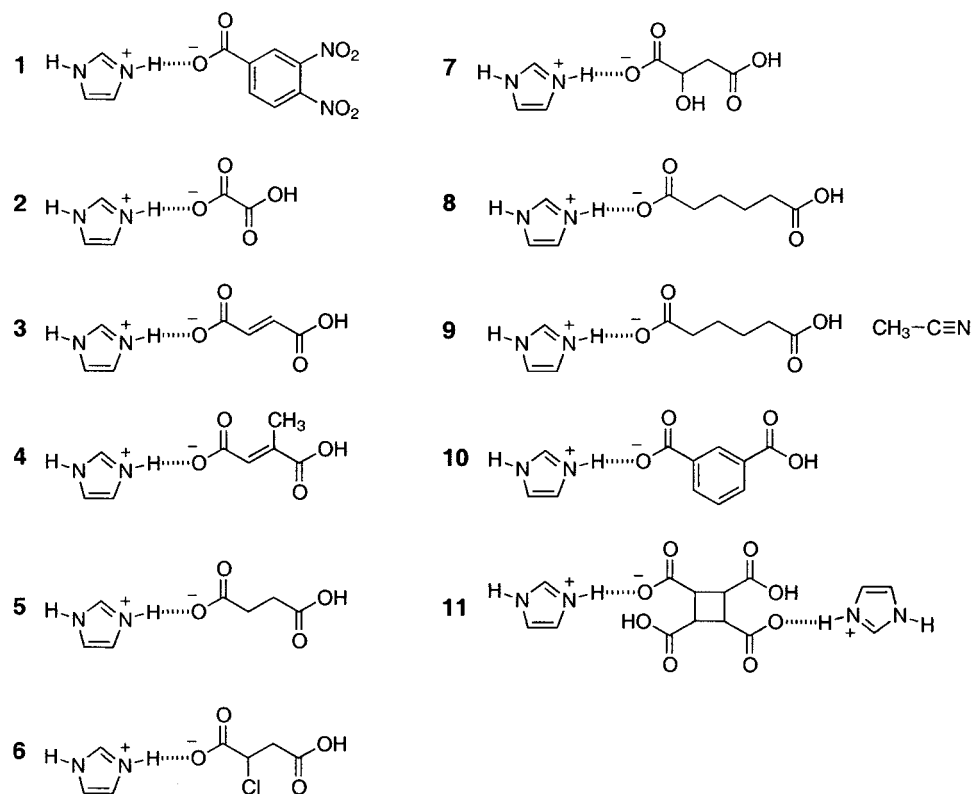


Figure 1. Structures of imidazolium carboxylate salts 1–11.

carboxylate anions, which we refer to as motif A, are shown schematically in Figure 2a. An example of motif A is shown in Figure 3 for imidazolium 3,4-dinitrobenzoate (**1**). Motif A is ubiquitous in imidazolium carboxylate salts because the hydrogen-bonding donors and acceptors reside separately on the cations and anions, respectively. Another reason we chose to work with imidazolium carboxylate salts is that motif A forms reliably; this is the only pattern of hydrogen bonds that can form when the ions self-assemble. Previous studies have shown that the monoanions of dicarboxylic acids also form hydrogen-bonded chains.^{35–38} The anions in these chains align head-to-tail and are joined by strong O–H···O hydrogen bonds. These chains of anions, which we refer to as motif B, are shown schematically in Figure 2b. We chose salts of dicarboxylic acids because the monoanions of dicarboxylic acids self-assemble by forming motif B exclusively. One feature that is common in motifs A and B is that the carboxylate group functions as the only hydrogen-bonding acceptor. Although the oxygen atom on the carboxyl group also can accept hydrogen bonds, the negatively charged carboxylate group is the stronger acceptor.³⁹ Our strategy in using salts between imidazole and dicarboxylic acids was to create building blocks capable of forming motifs A and B simultaneously, as shown schematically in Figure 2c. We anticipated that intersection of the two types of chains at the anions would generate layers. Finally, we wanted to develop building blocks that were useful not only to engineer structure but also to control and modify the physical properties of the resulting crystalline solids. The salts of imidazole and dicarboxylic acids are ideal in that respect because they are composed of two interchangeable components and, thus, are modular.

Results and Discussion

Noncrystallographic Characterization of Imidazolium Carboxylate Salts. Reaction of imidazole with 1 molar equiv of mono-, di-, or tetracarboxylic acid in solution, followed by evaporation of solvent or vapor diffusion, gave crystals of **1–11**. Since the carboxylic acids in **2–10** contained two CO₂H groups (four CO₂H groups in **11**), deprotonation of the acids by imidazole could occur more than once. The relative molar ratios of the two components were determined by ¹H NMR and later confirmed from the crystal structures. All complexes formed 1:1 imidazolium carboxylate salts except for **11**, which formed a 2:1 bis(imidazolium) dicarboxylate salt. Addition of 2 molar equiv of imidazole to solutions that contained just 1 molar equiv of succinic acid or adipic acid gave crystals of **5** and **8**, respectively, and also crystals of pure imidazole. Although we have not repeated this experiment with any of the other dicarboxylic acids, this result suggests that the pK_a values of the remaining carboxyl groups on the monoanions of the dicarboxylic acids in **2–4**, **6**, **7**, **9**, and **10** may be high enough to prevent deprotonation by a second 1 equiv of imidazole. Deprotonation of both carboxyl groups by 2 equiv of imidazole would produce bis(imidazolium)dicarboxylate salts and thus preclude the formation of motif B. Deprotonation did occur on two of the four carboxyl groups of 1,2,3,4-cyclobutanetetracarboxylic acid in **11** when 2 equiv of imidazole was added. We did not add excess imidazole to determine whether deprotonation would occur at more than two of the four carboxyl groups on 1,2,3,4-cyclobutanetetracarboxylic acid.

Solid-state infrared spectroscopy was used to confirm that proton transfer from the carboxylic acid to imida-

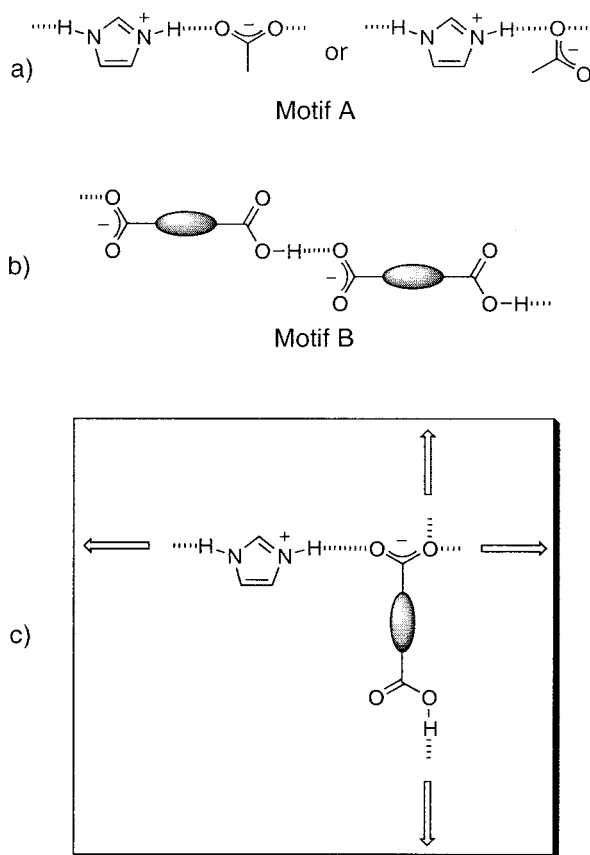


Figure 2. Illustration of different motifs of hydrogen bonds formed by imidazolium carboxylate salts: (a) hydrogen-bonded chain composed of alternating imidazolium cations and carboxylate anions (motif A); (b) hydrogen-bonded chain composed of monoanions of dicarboxylic acids (motif B); (c) imidazolium carboxylate building block that combines motifs A and B to generate hydrogen-bonded layers.

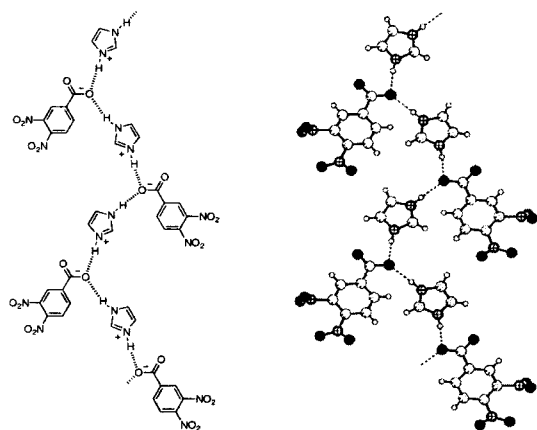


Figure 3. Example of a hydrogen-bonded chain of alternating imidazolium cations and carboxylate anions (motif A) formed in the crystal structure of imidazolium 3,4-dinitrobenzoate (**1**).

zole occurred and to identify the presence of specific hydrogen bonds. These data complemented the X-ray crystal structures for **2–11** by confirming the presence of CO_2H and CO_2^- groups on the anions. A set of infrared spectra for **6** that is typical for **2–11** is shown in Figure 4. Proton transfer in **2–11** was confirmed by a reduction in the intensity of carboxyl $\text{C}=\text{O}$ stretching bands between 1673 and 1737 cm^{-1} (Figure 4c, peak *ii*)

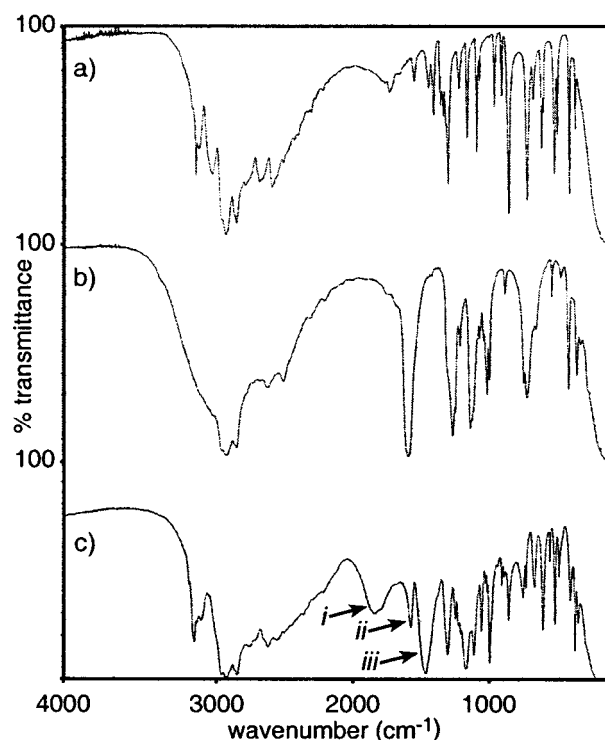


Figure 4. Comparison of solid-state (Nujol) infrared spectra of (a) imidazole, (b) 2-chlorosuccinic acid, and (c) imidazolium hydrogen 2-chlorosuccinate (**6**). Peak assignments for (c): (*i*) N–H stretch of the imidazolium cation; (*ii*) carbonyl stretch of the CO_2H group; (*iii*) antisymmetric C–O stretch of the CO_2^- group.

that were present in the spectra of the corresponding neutral carboxylic acids and by the appearance of carboxylate antisymmetric C–O stretching bands between 1592 and 1650 cm^{-1} (Figure 4c, peak *iii*). The presence of weak carbonyl stretching bands between 1673 and 1737 cm^{-1} (Figure 4c, peak *ii*) in the spectra of **2–11** indicated that at least one CO_2H group remained in the neutral form. Imidazolium N–H stretching frequencies are sensitive to hydrogen bonding and to the electronic nature of the acceptor atom to which the N–H group is bonded. In its own crystal structure, neutral imidazole forms $\text{N–H}\cdots\text{N}$ hydrogen-bonded chains that give a low-frequency N–H stretching band at 1834 cm^{-1} (Figure 4a). After proton transfer, formation of strong $\text{N–H}\cdots\text{O}$ hydrogen bonds gave a broad low-frequency band between 1870 and 2003 cm^{-1} in the spectra of **1–11** (Figure 4c, peak *i*). This band appeared in a frequency range similar to that reported for N–H \cdots O stretching bands of pyridinium carboxylate salts.⁴⁰

N–H \cdots O and O–H \cdots O Hydrogen Bonds and Formation of Chains. Imidazolium cations and carboxylate anions self-assembled via $\text{N–H}\cdots\text{O}$ hydrogen bonds to form chains with motif A (Figure 2). Motif A formed in **2–4** and **6–11**, despite the presence of competing hydrogen-bonding acceptors such as carboxyl and hydroxyl groups. This hydrogen-bonding arrangement used only two of the lone pairs of electrons on the carboxylate groups; consequently, carboxylate groups were free to accept additional hydrogen bonds. Salt **5** featured a slightly different pattern of hydrogen bonds in which the imidazolium cations bonded to both carboxylate anions and neutral carboxyl groups. This

connectivity gave a variation of motif A in which the repeat unit of the chain incorporated the entire carbon backbone of the anion rather than just the carboxylate group. The N \cdots O and H \cdots O bond lengths ranged between 2.65 and 2.87 Å and between 1.79 and 2.01 Å with average lengths of 2.73 and 1.88 Å, respectively. The N–H \cdots O bond angles ranged between 155 and 176° with an average angle of 168°. These values are consistent with values reported from a statistical analysis of N–H \cdots O hydrogen bonds involving imidazolium residues in crystal structures that contained histidine⁴¹ and from a study of N–H \cdots O hydrogen bonding in salts of imidazole with monocarboxylic acids.³⁴

The anions in **2–11** formed O–H \cdots O hydrogen bonds in a head-to-tail arrangement that gave chains with motif B. Imidazole deprotonated one carboxyl group when crystallized with dicarboxylic acids (**2–10**) and two carboxyl groups when crystallized with a tetracarboxylic acid (**11**). For dicarboxylic acids that were substituted unsymmetrically (**4**, **6**, and **7**), the site of deprotonation could be predicted *a priori* based on the proximity and the electron-withdrawing or electron-donating capability of substituents. The O \cdots O and H \cdots O bond lengths ranged between 2.48 and 2.63 Å and 1.67 and 1.82 Å with average lengths of 2.56 and 1.75 Å, respectively. The O–H \cdots O bond angles ranged between 159 and 177° with an average angle of 171°.

Formation of Layers. The molecular and supramolecular structures of **2–11** are shown in Figure 5. Intersection of motifs A and B at the carboxylate groups of anions formed layers of molecules in all of these structures. These layers could be divided into four different types, I–IV, on the basis of differences in the connectivity of hydrogen bonds between the imidazolium carboxylate building blocks and on differences in the relative orientation of the chains defined by motifs A and B. Schematic representations of layers I–IV are shown in Figure 6. The differences between layers I–IV are best described by considering the relative orientation of the chains of anions and the symmetry relationships between the ion pairs within these chains. For example, layers I and II are similar in that the chains of anions align in a parallel arrangement with the carboxyl groups (represented by arrowheads in Figure 6) pointing in the same direction. Layers I and II differ because the ion pairs in layer I are related by translational symmetry, while those in layer II are related by screw or glide symmetry. While the alignment and symmetry relationships between ion pairs in layer IV are similar to those in layer II, the connectivity of the hydrogen bonds (dashed lines in Figure 6) between ion pairs in adjacent chains differs significantly. Layer III differs from layers I, II, and IV because the chains of anions are aligned in an antiparallel arrangement with the carboxyl groups (arrowheads) in adjacent chains pointing in opposite directions and related by screw symmetry.

Layers I–IV all lack centers of symmetry and thus form supramolecular networks that are polar. These layers should serve as polar scaffolds with which to generate polar crystalline materials for applications such as second-harmonic generation if a method is developed to align the layers during crystallization. For example, **7** exhibits modest second-order nonlinear

optical activity.⁴² Although we have not attempted to control the packing of layers in **2–11** in the third dimension, salts **7**, **8**, and **10** crystallize in noncentrosymmetric space groups and form crystals that are polar.

Imidazolium salts **3**, **4**, **6**, and **11** form layer I. Adjacent layers are related through inversion symmetry to give a centric crystal structure. Monoanions in **4** and **6** contain methyl and chlorine substituents, respectively, which tilt out of the plane of the layer on one side so that the substituents interleave in alternating layers. This arrangement forms bilayers within the crystal. Interestingly, crystals of **6** were grown from a racemic solution of chlorosuccinic acid that crystallizes with (2*R*)- and (2*S*)-chlorosuccinate monoanions segregated in adjacent layers so that each layer is homochiral. Bis-(imidazolium) 2,4-dihydrogen *cis,trans,cis,trans*-1,2,3,4-cyclobutanetetracarboxylate (**11**) is unique in that the halves of the dianion behave like the monoanions in salts **3**, **4**, and **6** by forming separate layers that are connected covalently through the center of the cyclobutane ring.

Molecules in **7** form layer II. Hydroxyl substituents at the 2-position of the hydrogen malate anions stick out of the layer on both sides and form a second set of O–H \cdots O hydrogen bonds to carboxylate groups in adjacent layers. These interactions link the layers together in the third dimension to form chiral crystals. These crystals exhibit nonlinear optical activity, as mentioned previously.

The salts in **2**, **8**, and **9** form layer III. The asymmetric unit in **8** contains two crystallographically independent pairs of ions that form crystallographically independent layers that are nearly identical in structure. The two layers stack in an alternating arrangement in which the layers are offset slightly so that imidazolium cations in one layer protrude into the gaps between the anions in adjacent layers. Salt **9** is a pseudopolymorph of **8** in which molecules of acetonitrile solvent are included in the lattice. The pairs of ions in **9** form layers similar in structure to those in **8**. Molecules of acetonitrile are trapped within each layer in the spaces between the anions. These guest molecules do not form hydrogen bonds with ions within or between layers. It is worth noting that molecules of acetonitrile in **9** occupy the void spaces in the layers that are filled in **8** by imidazolium cations that protrude from adjacent layers. The structure of **9** is the only example we have examined of a salt with anions long enough to create cavities in the layers that are large enough to accommodate molecules of solvent during crystallization. We currently are investigating salts with dicarboxylic acids that are longer than adipic acid to determine whether inclusion of guest molecules is a general phenomenon that can be exploited to trap guest molecules selectively.

Salt **10** is the only structure that forms layer IV. While the spatial orientation of molecules within this network is similar to that in network II, orientation of the hydrogen-bond chains in motifs A and B *parallel* to one another makes layer IV unique.

Effect of Hydrogen Bonding on the Geometry of Carboxylate Groups. While all carboxylate groups in **1–11** participate as hydrogen-bonding acceptors, the C–O bond lengths vary significantly with the number

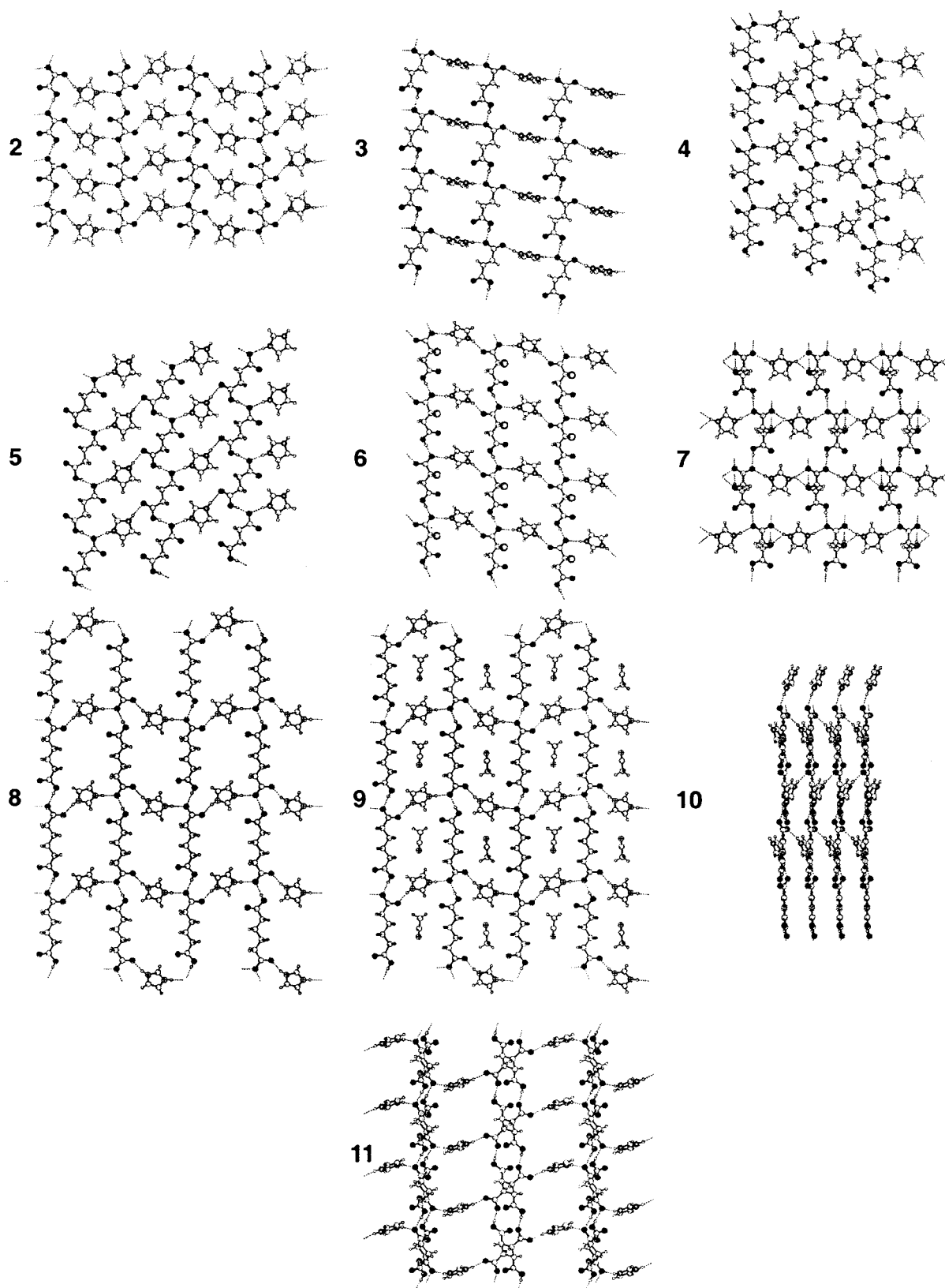


Figure 5. The different hydrogen-bonded layers formed by **2–11**.

and type of hydrogen-bonding donors bonded to the oxygen atom. In the absence of hydrogen bonding and other electronic perturbations, the C–O bond lengths should be equal because of resonance. The formation of single or multiple hydrogen bonds at one oxygen atom should cause the associated C–O bond to lengthen. The

differences in C–O bond lengths in carboxylate groups vary between 0.003 and 0.075 Å in **1–11**. The largest difference occurs in **5**, where a very short (2.48 Å) O–H...O hydrogen bond forms between the carboxyl and carboxylate groups. Salt **5** is unusual because it is the only structure in which the carboxyl and carboxylate

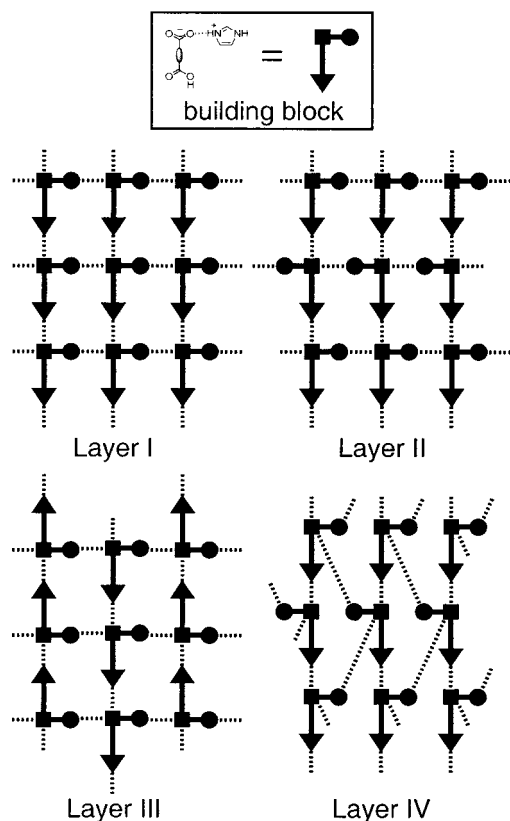


Figure 6. Schematic illustration of four different types of layers: (layer I) **3**, **4**, **6**, and **11**; (II) **7**; (III) **2**, **8**, and **9**; (IV) **10**. Dashed lines represent hydrogen bonds.

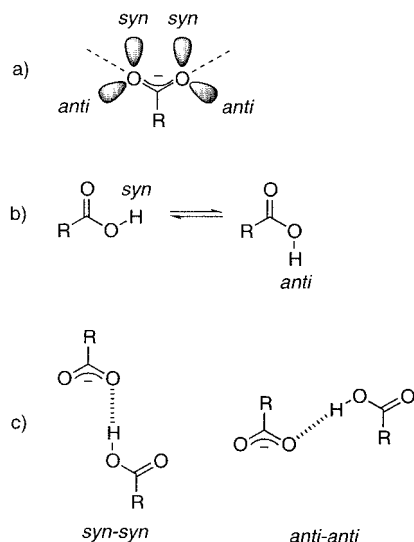


Figure 7. (a) *syn* and *anti* lone pairs of electrons on a carboxylate group. (b) *syn* and *anti* conformations of a carboxylic acid. (c) *syn-syn* and *anti-anti* hydrogen-bonding arrangements for a carboxylic acid and carboxylate group.

groups adopt an *anti-anti* arrangement, as shown in Figure 7. It is the only structure other than **1** in which the second carboxylate oxygen is not used in hydrogen bonding. The carboxyl groups all form longer O-H \cdots O hydrogen bonds (>2.5 Å) to the oxygen atoms on the longer C-O (0.010–0.052 Å) bond in **2–4** and **6–11**. Carboxyl and carboxylate groups adopt the *syn-syn* conformation in all of these structures, as shown in Figure 7. Both carboxylate oxygen atoms form strong

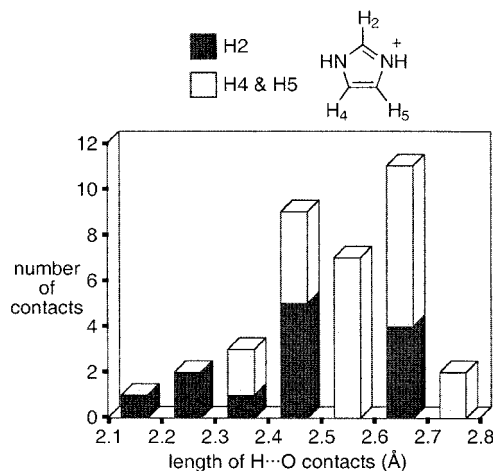


Figure 8. Bar graph that shows the distribution of H \cdots O distances from X-ray data for 35 C-H \cdots O contacts formed by 12 different imidazolium cations in the crystal structures of **1–11**. Only those C-H \cdots O contacts with H \cdots O distances less than the sum of the van der Waals radii for hydrogen (1.20 Å)⁴³ and oxygen (1.52 Å)⁴³ are shown.

N-H \cdots O hydrogen bonds with imidazolium cations. Each carboxylate group accepts a combined total of at least three O-H \cdots O and N-H \cdots O hydrogen bonds.

Role of Weak Hydrogen Bonds in Defining Supramolecular Assembly. A previous study of C-H \cdots O hydrogen bonds in crystals of organic compounds demonstrated that nitrogen atoms decrease electron density at adjacent C-H protons inductively, thereby enhancing the ability of C-H protons to act as hydrogen-bonding donors. We anticipated that the formation of C-H \cdots O hydrogen bonds would influence molecular packing in **1–11**, since every carbon atom in an imidazolium cation is bonded to one or two nitrogen atoms and also because **1–11** have a high ratio of oxygen to carbon. Consequently, we examined all intermolecular contacts between C-H protons on 12 crystallographically unique imidazolium cations and neighboring oxygen atoms. All of these interactions had H \cdots O distances less than 2.72 Å (the sum of the van der Waals radii for hydrogen (1.20 Å)⁴³ and oxygen (1.52 Å)⁴³) and C-H \cdots O angles greater than 90°. The H \cdots O distances were examined rather than the C \cdots O distances because most of the C-H \cdots O interactions were bent instead of linear. The distribution of H \cdots O bond lengths is shown in Figure 8.

The 12 imidazolium cations had 31 C-H protons (86%) that formed 35 C-H \cdots O hydrogen bonds with oxygen atoms on carboxylate C-O, carboxyl C=O, carboxyl OH, alkyl OH, and NO₂ groups. Of these, 27 C-H protons formed one C-H \cdots O contact and 4 formed two C-H \cdots O contacts. The H \cdots O bond lengths ranged between 2.15 and 2.70 Å with an average length of 2.52 Å. The C-H \cdots O bond angles ranged between 108 and 178° with an average angle of 140°. The fact that most of the C-H \cdots O interactions deviated significantly from linearity is not surprising, considering that formation of stronger N-H \cdots O hydrogen bonds is one of the principal organizational forces involved in determining the orientation of imidazolium cations during crystal packing. We anticipated that H \cdots O contacts involving protons C2 would be shorter and occur with greater frequency than those involving protons on C4 and C5, since C2 is bonded to nitrogen atoms on both sides,

while C4 and C5 are bonded to nitrogen atoms once. Protons on C2 form 37% of the H \cdots O contacts, and protons on C4 and C5 form 63% of the H \cdots O contacts, as shown in Figure 8. Although the frequency of contacts with protons on C2, C4, and C5 is nearly statistical, the shortest contacts form predominantly with protons on C2, as expected.

It is important to point out that the H \cdots O distances in **1–11** were determined on the basis of X-ray data in which all of the C–H hydrogen atoms on imidazolium cations were placed at idealized positions 0.93 Å from the carbon atom to which they were bonded during refinement of the crystal structures. Hydrogen atoms were treated in this manner because the positions of hydrogen atoms cannot be determined accurately with X-ray diffraction, especially with data collected at room temperature. Consequently, the H \cdots O distances in **1–11** most likely are shorter than the distances reported here. For example, data on C–H bond lengths from studies using neutron diffraction suggest that C–H bond lengths should be fixed at 1.08 Å for organic compounds. Considering that the SHELXL-93 refinement program⁴⁴ assigns the shorter distance of 0.93 Å for C–H bond lengths on aromatic compounds, the H \cdots O distances in **1–11** are probably as much as 0.15 Å shorter than the values we have reported. Moreover, since the C–H bond distances in **1–11** were not fixed at 1.08 Å, our data do not include a number of longer C–H \cdots O contacts that would have H \cdots O bond lengths less than the cutoff of 2.72 Å and qualify as C–H \cdots O hydrogen bonds.

The shortest H \cdots O contact occurs in the structure of **5**. The imidazolium cations are coplanar with the hydrogen-bonded layer in this structure. Each cation is surrounded by six oxygen atoms that form an acceptor-rich pocket, as shown in Figure 9. Within the pocket, protons on C2 (C in Figure 9a) form short, nearly linear C–H \cdots O hydrogen bonds (X-ray data: C \cdots O = 3.08 Å, H \cdots O = 2.15 Å, C–H \cdots O = 176°) to oxygen atoms on carboxylate groups. The neutron crystal structure of **5** also was solved to determine the positions of the protons accurately (neutron data: C \cdots O = 3.07 Å, H \cdots O = 1.99 Å, C–H \cdots O = 175°).⁴⁵ Lengthening of the H \cdots O distance for the proton on C2 by 0.16 Å on going from the X-ray data to the neutron data is consistent with the discussion in the previous paragraph regarding the accuracy of the X-ray data. This C–H \cdots O interaction is nearly linear, with a C \cdots O distance comparable to N \cdots N and N \cdots O distances reported for N–H \cdots N and N–H \cdots O interactions for organic compounds.⁴⁶ Protons on C4 and C5 (D and E in Figure 9a) are directed between pairs of oxygen atoms on carboxylate and carboxyl groups, where they form three-centered interactions. The imidazolium cations in this structure function as multidentate hydrogen-bonding donors in which all of the protons on the cations form at least one C–H \cdots O hydrogen bond with oxygen atoms *within* the layer, as shown schematically in Figure 10a. van der Waals interactions appear to be the dominant interaction *between* layers in **5**. It is interesting to note that in order to surround the imidazolium cation with six oxygen atoms, the carboxyl and carboxylate groups must adopt the *anti–anti* conformation (Figure 7) in order for the anions to form O–H \cdots O hydrogen bonds that generate motif B. The *anti–anti* conformation is less common

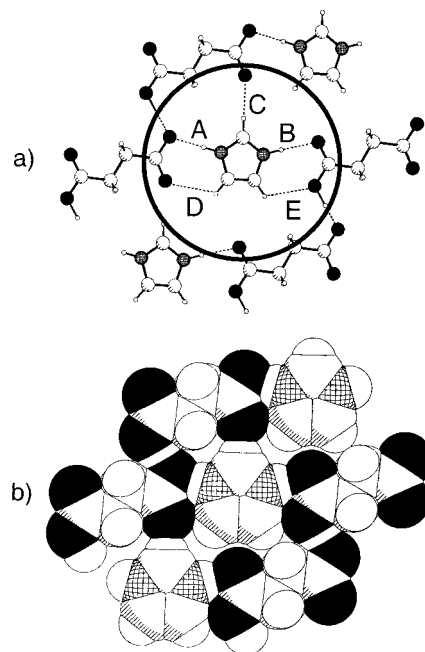


Figure 9. (a) All five of the hydrogen atoms on imidazolium cations in **5** participating in forming hydrogen bonds with oxygen atoms on neighboring hydrogen succinate anions. H \cdots O (neutron data): A = 1.66 Å, B = 1.82 Å, C = 1.99 Å, D = 2.49 Å, and E = 2.46 Å. (b) Space-filling model that shows how imidazolium cations sit in an electron-rich pocket surrounded by six oxygen atoms (black).

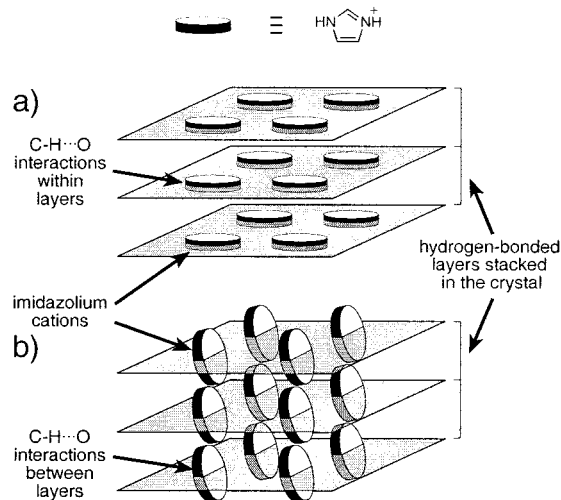


Figure 10. Schematic illustration that shows the orientation of imidazolium cations relative to the stacking of hydrogen-bonded layers: (a) imidazolium cations coplanar with the hydrogen-bonded layers so that C–H \cdots O interactions occur within layers (e.g., **5**); (b) imidazolium cations twisted out of the plane of the hydrogen-bonded layers so that C–H \cdots O interactions occur between adjacent layers (e.g., **2–4** and **6–11**).

than the *syn–syn* conformation for hydrogen bonds between carboxyl and carboxylate groups.^{37,38}

The imidazolium cations in **1–4** and **6–11** also function as multidentate hydrogen-bonding donors by forming two or three C–H \cdots O hydrogen bonds in addition to forming the two N–H \cdots O hydrogen bonds in motif A. The cations in **2–4** and **6–11** are not coplanar with the layers but, instead, are twisted out of the plane of the layer, as shown schematically in

Figure 10b. This twisting of the cations causes the protons on C2 to project outward from one side of a given layer and the protons on C4 and C5 to project outward from the opposite side of the layer. Consequently, the imidazolium cations in **2–4** and **6–11** generally form C–H \cdots O interactions between layers instead of within layers. One reason the cations may twist out of the layers in these structures is to maximize the number of C–H \cdots O contacts that form. Visual inspection and molecular modeling of individual layers in **2–4** and **6–11** suggest that fewer C–H \cdots O interactions would occur if the cations were coplanar with the layers in these structures. In the case of **4**, **6**, and **7**, the cations must twist to avoid steric repulsion from the methyl, chloro, and hydroxyl substituents on the anions, respectively.

Conclusions

Imidazolium carboxylate salts of dicarboxylic acids form polar hydrogen-bonded layers composed of intersecting chains of N–H \cdots O and O–H \cdots O hydrogen bonds. Four different layers were identified that serve as scaffolds with which to control molecular packing in two dimensions. In these structures, carboxylate anions function as acceptors for multiple hydrogen bonds that organize and orient imidazolium cations and carboxylate anions in two dimensions. Imidazolium cations function as multidentate hydrogen-bonding donors that cross-link chains of anions and that form multiple C–H \cdots O hydrogen bonds which link anions in adjacent layers. Layers based on imidazolium carboxylate salts should prove useful for engineering the structures of crystals, because these systems are modular. This modularity is ideal for the design of crystalline solids, because it enables a range of different substituted dicarboxylic acids to be introduced to alter the properties of these materials without disrupting the formation of layers.

Experimental Section

General Considerations. All chemicals and solvents were purchased from Aldrich or ACROS and used as received without further purification. Melting points were determined on a Fisher-Johns apparatus and are uncorrected. Infrared spectra were recorded on a Nicolet 5DXB FTIR spectrometer from Nujol mulls unless otherwise indicated and are reported in cm^{-1} . ^1H NMR spectra were recorded on an IBM NR200AF spectrometer from solutions in d_6 -DMSO, and chemical shifts are reported in parts per million (δ) from TMS. Spectroscopic grade solvents were used for all experiments involving crystallization.

Methods for Preparing Crystals between Imidazole and Carboxylic Acids (1–11). Salts of imidazole and carboxylic acids were prepared in solution. Crystals of these salts were obtained by using one of two techniques. Method A (slow evaporation): equimolar amounts of imidazole and carboxylic acid were dissolved in a single solvent or solvent mixture. The solution was left uncovered and allowed to evaporate slowly at room temperature until crystals appeared. Crystals were removed from solution before the solvent evaporated completely in order to isolate pure single crystals. Method B (vapor diffusion): equimolar amounts of imidazole and carboxylic acid were dissolved in a solvent in which both components were soluble. A beaker of this solution was placed inside a wide-mouth jar containing a second precipitating solvent in which the imidazole and carboxylic acid were insoluble. Crystals formed slowly over days or weeks as the precipitating solvent diffused into the solution of the imidazole and carboxylic acid. Crystals were removed as they grew.

The experimental data for each imidazolium salt are listed in the following order: compound name (number); color of crystal and morphology, crystallization method (solvent system); melting point; IR (cm^{-1}); ^1H solution NMR (frequency, solvent) chemical shift (ppm), and multiplicity.

Determination of X-ray Crystal Structures. X-ray diffraction data on single crystals were collected on an Enraf-Nonius CAD4 diffractometer with graphite-monochromated Mo K α radiation ($\lambda = 0.71069$) using the ω - 2θ technique. Lattice parameters were obtained from least-squares analysis of 25 reflections. SHELXS-86 and SHELXL-93 software were used to solve and refine structures on an SGI O2 UNIX platform. Refinement was based on F^2 . All non-hydrogen atoms were refined anisotropically. All hydrogen atoms on heteroatoms were first located in difference maps and then fixed in calculated positions and refined isotropically with thermal parameters based upon the corresponding attached heteroatoms ($U(\text{H}) = 1.2[U_{\text{eq}}(\text{C})]$). The remaining hydrogen atoms were fixed in calculated positions and refined isotropically with thermal parameters based upon the corresponding attached carbon atoms ($U(\text{H}) = 1.2[U_{\text{eq}}(\text{C})]$). Crystal data and details of the structure determination and refinement are given in Table 1.

Imidazolium 3,4-Dinitrobenzoate (1): yellow blocks; method A (1:1 methanol/toluene); mp 163–167 °C; IR (Nujol) 3156, 3114, 2600, 1975, 1625, 1595, 1552, 1364, 1339, 1332, 868, 848, 819, 782, 767, 740, 723, and 641 cm^{-1} ; ^1H NMR (200 MHz, d_6 -DMSO) δ 7.43 (s, 2 H), 8.25 (d, 1 H), 8.45 (m, 3 H), and 14.59 (br s, 2 H).

Imidazolium Hydrogen Oxalate (2): colorless blocks; method A (2:1 ethanol/water); mp 249–251 °C; IR (Nujol) 3163, 3142, 3064, 2636, 1891, 1795, 1734, 1611, 1586, 1452, 1326, 1226, 1132, 1105, 1067, 1025, 975, 904, 841, 711, and 630 cm^{-1} .

Imidazolium Hydrogen Fumarate (3): colorless prisms; method A (methanol); mp 175–180 °C; IR (Nujol) 3156, 3114, 2600, 1982, 1697, 1641, 1590, 1293, 1279, 1223, 1062, 988, 929, 894, 751, 643, and 629 cm^{-1} ; ^1H NMR (200 MHz, d_6 -DMSO) δ 6.62 (s, 2 H), 7.14 (s, 2 H), 7.91 (s, 1 H), and 11.81 (br s, 3 H).

Imidazolium Hydrogen Mesaconate (4): colorless plates; method A (1:1 methanol/acetonitrile); mp 167–170 °C; IR (Nujol) 3149, 3114, 2600, 1905, 1696, 1649, 1599, 1393, 1366, 1331, 1295, 1253, 1199, 1130, 1089, 1019, 938, 898, 850, 778, 674, 644, and 635 cm^{-1} ; ^1H NMR (200 MHz, d_6 -DMSO) δ 2.13 (s, 3 H), 6.61 (s, 1 H), 7.16 (s, 2 H), 7.95 (s, 1 H), and 12.96 (s, 3 H).

Imidazolium Hydrogen Succinate (5): colorless blocks; method A (1:1 methanol/acetonitrile); mp 141–144 °C; IR (Nujol) 3177, 3107, 2600, 1919, 1689, 1632, 1598, 1461, 1416, 1047, 944, 884, 809, 770, and 738 cm^{-1} ; ^1H NMR (200 MHz, d_6 -DMSO) δ 2.42 (s, 4 H), 7.09 (s, 2 H), 7.80 (s, 1 H), and 12.34 (br s, 3 H).

Imidazolium Hydrogen 2-Chlorosuccinate (6): tan prisms; method A (1:1 methanol/acetonitrile); mp 134–137 °C; IR (Nujol) 3149, 3093, 2650, 1940, 1701, 1602, 1460, 1344, 1291, 1241, 1167, 1064, 990, 841, 762, 662, and 631 cm^{-1} ; ^1H NMR (200 MHz, d_6 -DMSO) δ 2.79 (dd, 1 H), 2.97 (dd, 1 H), 4.53 (t, 1 H), 7.35 (s, 2 H), 8.38 (s, 1 H) and 13.68 (s, 3 H).

Imidazolium Hydrogen (2R)-Malate (7): colorless thin plates; method A (methanol); mp 121–123 °C; IR (Nujol) 3248, 3149, 3100, 2600, 1884, 1716, 1599, 1581, 1458, 1416, 1326, 1277, 1237, 1191, 1179, 1097, 1057, 851, 768, 681, and 635 cm^{-1} ; ^1H NMR (200 MHz, d_6 -DMSO) δ 2.41 (dd, 1 H), 2.62 (dd, 1 H), 4.20 (dd, 1 H), 7.20 (s, 2 H), 8.05 (s, 1 H), and 11.07 (br s, 4 H).

Imidazolium Hydrogen Adipate (8): colorless blocks; method A (methanol); mp 101.5–103 °C; IR (Nujol) 3149, 3121, 2550, 1954, 1706, 1604, 1548, 1414, 1336, 1287, 1243, 1191, 894, 852, and 637 cm^{-1} ; ^1H NMR (200 MHz, d_6 -DMSO) δ 1.48 (s, 4 H), 2.19 (s, 4 H), 7.02 (s, 2 H), 7.67 (s, 1 H), and 11.31 (br s, 2 H).

Imidazolium Hydrogen Adipate Acetonitrile Solvate (9): colorless prisms; method A (1:1 methanol/acetonitrile); mp 101–103 °C; IR (Nujol) 3149, 3121, 2580, 1954, 1706, 1604, 1548, 1462, 1414, 1287, 1242, 1191, 894, 852, and 637 cm^{-1} ; ^1H NMR (200 MHz, d_6 -DMSO) δ 1.50 (pent, 5 H), 2.08 (s, 3

Table 1. Collection of X-ray Data and Refinement of Crystal Structures for 1–11

	1	2	3	4	5	6	7	8	9	10	11
formula	C ₁₀ H ₈ N ₄ O ₆	C ₃ H ₆ N ₂ O ₄	C ₇ H ₈ N ₂ O ₄	C ₈ H ₁₀ N ₂ O ₄	C ₇ H ₁₀ N ₂ O ₄	C ₇ H ₉ N ₂ O ₄ Cl	C ₇ H ₁₀ N ₂ O ₅	C ₇ H ₁₄ N ₂ O ₄	C ₁₁ H ₁₇ N ₃ O ₄	C ₁₁ H ₁₀ N ₂ O ₄	C ₁₄ H ₁₆ N ₄ O ₈
fw	280.20	158.12	184.15	198.18	186.17	220.16	202.17	184.15	255.28	234.21	368.31
temp (K)	298(1)	298(1)	297(2)	297(2)	297(2)	297(2)	297(2)	297(2)	297(2)	297(2)	297(2)
cryst syst	monoclinic	monoclinic	triclinic	triclinic	triclinic	triclinic	orthorhombic	orthorhombic	monoclinic	orthorhombic	orthorhombic
space group	P2 ₁ /c	P2 ₁ /n	P1	P1	P1	P1	P2 ₁ 2 ₁ 2 ₁	Pna2 ₁	P2 ₁ /n	P2 ₁ 2 ₁ 2 ₁	Pbca
a (Å)	8.133(2)	5.688(4)	7.478(2)	6.849(2)	6.583(2)	8.084(3)	6.660(1)	17.021(4)	10.764(5)	3.883(2)	7.666(8)
b (Å)	11.088(2)	17.513(4)	7.747(2)	8.043(2)	7.421(3)	8.253(5)	9.216(4)	10.679(3)	16.688(4)	14.015(2)	12.070(3)
c (Å)	13.136(2)	6.810(2)	8.416(2)	8.917(2)	9.648(2)	8.990(5)	14.653(3)	12.076(5)	7.624(3)	19.302(2)	16.864(3)
α (deg)	90	90	69.69(2)	100.63(2)	67.89(3)	101.10(5)	90	90	90	90	90
β (deg)	93.42(2)	105.55(4)	81.42(2)	105.15(2)	73.91(2)	107.72(4)	90	90	101.60(3)	90	90
γ (deg)	90	90	66.18(2)	100.16(2)	81.40(3)	117.47(4)	90	90	90	90	90
V (Å ³)	1182.4(7)	653.6(5)	418.2(2)	452.7(2)	419.0(2)	465.9(4)	899.3(5)	2195(1)	1341.5(9)	1050.4(6)	1560(2)
Z	4	4	2	2	2	2	4	8	4	4	4
D _{calc} (g/cm ³)	1.57	1.61	1.46	1.45	1.48	1.57	1.49	1.30	1.26	1.48	1.57
R1/wR2 (obsd)	0.0476/	0.0443/	0.0420/	0.0562/	0.0435/	0.0781/	0.0845/	0.0503/	0.0651/	0.0387/	0.0424/
data: I > 2σ(I) ^a	0.1212	0.1134	0.1213	0.1473	0.1382	0.2066	0.1949	0.0980	0.1365	0.0983	0.1051
R1/wR2	0.0625/	0.0543/	0.0575/	0.0685/	0.0505/	0.0939/	0.0952/	0.0878/	0.1132/	0.0434/	0.0581/
(all data) ^a	0.1296	0.1209	0.1333	0.1572	0.1443	0.2197	0.2047	0.1135	0.1586	0.1017	0.1137
goodness of fit on F ²	1.047	1.035	1.048	1.061	1.031	1.088	1.111	0.948	1.011	1.109	1.051

$$^a R1 = \sum(|F_o| - |F_c|)/\sum|F_o|; wR2 = [\sum w(|F_o| - |F_c|)^2/\sum w(F_o)^2]^{1/2}.$$

H), 2.20 (t, 4 H), 7.04 (s, 2 H), and 7.68 (s, 1 H). Upon removal from solvent, crystals slowly lose solvent and turn opaque after 24 h.

Imidazolium Hydrogen Isophthalate (10): colorless rods; method B (methanol/toluene); mp 193–198 °C; IR (Nujol) 3170, 3100, 2640, 1900, 1717, 1608, 1560, 1459, 1325, 1304, 1243, 1161, 1078, 736, 683, and 630 cm⁻¹; ¹H NMR (200 MHz, d₆-DMSO) δ 7.14 (s, 2 H), 7.63 (t, 1 H), 7.69 (s 1 H), 8.12 (m, 2 H), 8.52 (s, 1 H), and 9.62 (br s, 3 H).

Bis(imidazolium) 2,4-Dihydrogen *cis,trans,cis,trans*-1,2,3,4-Cyclobutanetetracarboxylate (11): crystals were obtained from a 2:1 solution of imidazole and acid; colorless prisms; method B (water/acetone); mp 195–200 °C; IR (Nujol) 3156, 3072, 2600, 1926, 1720, 1593, 1564, 1457, 1315, 1215, 1201, 1057, 1030, 1001, 897, 837, 811, 773, and 630 cm⁻¹; ¹H NMR (200 MHz, d₆-DMSO) δ 3.43 (s, 4 H), 7.13 (s, 4 H), 7.88 (s, 2 H), and 11.54 (br s, 6 H).

Acknowledgment is made to the donors of the Petroleum Research Fund, administered by the American Chemical Society, for support of this research at Northern Arizona University. J.C.M. dedicates this paper in memory of Margaret C. Etter. Special thanks are given to Doyle Britton at the University of Minnesota for collecting X-ray data on crystals of **1–11** and to Rob Henning and Art Schultz at the Intense Pulsed Neutron Source at Argonne National Laboratory for collecting the neutron diffraction data on crystals of **5**.

Supporting Information Available: X-ray crystallographic data are given in Tables S1–S58 for **1–11**. This material is available free of charge via the Internet at <http://pubs.acs.org>.

References

- (1) Desiraju, G. R. *Crystal Engineering: The Design of Organic Solids*; Elsevier: New York, 1989; Vol. 54.
- (2) Wright, J. D. *Molecular Crystals*; Cambridge University Press: Cambridge, U.K., 1987.
- (3) Luo, T.-J. M.; Palmore, G. T. R. *J. Phys. Org. Chem.*, in press.
- (4) Palmore, G. T. R.; Luo, T.-J. M.; Martin, T. L.; McBride-Wieser, M. T.; Voong, N. T.; Land, T. A.; DeYoreo, J. J. *Trans. Am. Crystallogr. Assoc.* **1998**, *33*, 45–57.
- (5) Chin, D. N.; Zerkowski, J. A.; MacDonald, J. C.; Whitesides, G. M. In *Organised Molecular Assemblies in the Solid State*; Whitesell, J. K., Ed.; Wiley: New York, 1999; pp 185–253.
- (6) Coe, S.; Kane, J. J.; Nguyen, T. L.; Toledo, L. M.; Wininger, E.; Fowler, F. W.; Lauher, J. W. *J. Am. Chem. Soc.* **1997**, *119*, 86–93.
- (7) Ducharme, Y.; Wuest, J. D. *J. Org. Chem.* **1988**, *53*, 5787–5789.
- (8) Foxman, B. M.; Guarrera, D. J.; Taylor, L. D.; VanEngen, D.; Warner, J. C. *Cryst. Eng.* **1998**, *1*, 109–118.
- (9) Geib, S. J.; Vicent, C.; Fan, E.; Hamilton, A. D. *Angew. Chem., Int. Ed. Engl.* **1993**, *32*, 119–121.
- (10) Harris, K. D. M.; Stainton, N. M.; Callan, A. M.; Howie, R. A. *J. Mater. Chem.* **1993**, *3*, 947–952.
- (11) Hollingsworth, M. D.; Santarsiero, B. D.; Oumar-Mahamat, H.; Nichols, C. J. *Chem. Mater.* **1991**, *3*, 23–25.
- (12) Kane, J. J.; Liao, R.-F.; Lauher, J. W.; Fowler, F. W. *J. Am. Chem. Soc.* **1995**, *117*, 12003–12004.
- (13) Karle, I. L.; Ranganathan, D.; Haridas, V. *J. Am. Chem. Soc.* **1996**, *118*, 7128–7133.
- (14) Karle, I. L.; Ranganathan, D.; Haridas, V. *J. Am. Chem. Soc.* **1997**, *119*, 9, 2777–2783.
- (15) Lehn, J.-M.; Mascal, M.; DeCian, A.; Fischer, J. *J. Chem. Soc., Chem. Commun.* **1990**, 479–481.
- (16) MacDonald, J. C.; Whitesides, G. M. *Chem. Rev.* **1994**, *94*, 2383–2420.
- (17) MacDonald, J. C.; Dorrestein, P. C.; Pilley, M. M.; Foote, M. M.; Lundburg, J. L. *J. Am. Chem. Soc.*, in press.
- (18) Mascal, M.; Fallon, P. S.; Batsanov, A. S.; Heywood, B. R.; Champ, S.; Colclough, M. *J. Chem. Soc., Chem. Commun.* **1995**, 805–806.

- (19) Palacin, S.; Chin, D. N.; Simanek, E. E.; MacDonald, J. C.; Whitesides, G. M.; McBride, M. T.; Palmore, G. T. R. *J. Am. Chem. Soc.* **1997**, *119*, 11807–11816.
- (20) Palmore, G. T. R.; McBride, M. T. *Chem. Commun.* **1998**, 145–146.
- (21) Palmore, G. T. R.; Luo, T.-J. M.; McBride-Weiser, M. T.; Picciotto, E. A.; Reynoso-Paz, C. M. *Chem. Mater.* **1999**, *11*, 3315–3328.
- (22) Palmore, G. T. R.; MacDonald, J. C. In *The Amide Linkage: Structural Significance in Chemistry, Biochemistry and Materials Science*; Greenberg, A., Breneman, C. M., Liebman, J. F., Eds.; Wiley: New York, 2000; pp 291–336.
- (23) Pedireddi, V. R.; Chatterjee, S.; Ranganathan, A.; Rao, C. N. R. *J. Am. Chem. Soc.* **1997**, *119*, 10867–10868.
- (24) Schwiebert, K. E.; Chin, D. N.; MacDonald, J. C.; Whitesides, G. M. *J. Am. Chem. Soc.* **1996**, *118*, 4018–4029.
- (25) Simanek, E. E.; Tsoi, A.; Wang, C. C. C.; Whitesides, G. M.; McBride, M. T.; Palmore, G. T. R. *Chem. Mater.* **1997**, *9*, 1954–1961.
- (26) Toledo, L. M.; Lauher, J. W.; Fowler, F. W. *Chem. Mater.* **1994**, *6*, 1222–1226.
- (27) Zerkowski, J. A.; MacDonald, J. C.; Seto, C. T.; Wierda, D. A.; Whitesides, G. M. *J. Am. Chem. Soc.* **1994**, *116*, 2382–2391.
- (28) Zerkowski, J. A.; MacDonald, J. C.; Whitesides, G. M. *Chem. Mater.* **1994**, *6*, 1250–1257.
- (29) Zhao, X.; Chang, Y.-L.; Fowler, F. W.; Laughner, J. W. *J. Am. Chem. Soc.* **1990**, *112*, 6627–6634.
- (30) Leiserowitz, L. *Acta Crystallogr.* **1976**, *B32*, 775–802.
- (31) Bernstein, J. *J. Phys. D: Appl. Phys.* **1993**, *26*, B66–B76.
- (32) Zerkowski, J. A.; MacDonald, J. C.; Whitesides, G. M. *Chem. Mater.* **1997**, *9*, 1933–1941.
- (33) Chin, D. N.; Palmore, G. T. R.; Whitesides, G. M. *J. Am. Chem. Soc.* **1999**, *121*, 2115–2122.
- (34) Gandour, R. D.; Nabulsi, N. A. R.; Fronczek, F. R. *J. Am. Chem. Soc.* **1990**, *112*, 7816–7817.
- (35) Aakeröy, C. B.; Hitchcock, P. B.; Seddon, K. R. *J. Chem. Soc., Chem. Commun.* **1992**, 553–555.
- (36) Aakeröy, C. B.; Nieuwenhuyzen, M. *J. Am. Chem. Soc.* **1994**, *116*, 10983–10991.
- (37) Emsley, J. *Chem. Soc. Rev.* **1980**, *9*, 91.
- (38) Speakman, J. C. *Struct. Bonding* **1972**, *12*, 141.
- (39) Kamlet, M. J.; Abboud, J.-L. M.; Abraham, M. H.; Taft, R. W. *J. Org. Chem.* **1983**, *48*, 2877–2887.
- (40) Johnson, S. L.; Rumon, K. A. *J. Phys. Chem.* **1965**, *69*, 74.
- (41) Görbitz, C. H. *Acta Crystallogr.* **1989**, *B45*, 390.
- (42) Aakeröy, C. B. Personal communication.
- (43) Bondi, A. *J. Phys. Chem.* **1964**, *68*, 441.
- (44) Sheldrick, G. M. SHELXL-93; University of Göttingen, Göttingen, Germany, 1993.
- (45) A full description of the neutron crystal structure of **5** will be reported elsewhere: MacDonald, J. C.; Dorrestein, P. C.; Pilley, M. M.; Henning, R. W.; Schultz, A. J. Unpublished results.
- (46) Jeffrey, G. A.; Saenger, W. *Hydrogen Bonding in Biological Structures*; Springer-Verlag: Berlin, Heidelberg, New York, 1991.

CG000008K